Heavy-ion collisions and nuclear EOS

Akira Ono

Tohoku University

Advances and perspectives in computational nuclear physics
Octber 5 – 7, 2014, Hilton Waikoloa Village, Waikoloa, Hawaii

- Heavy-Ion Collisions (several ten - several hundred MeV/nucleon)

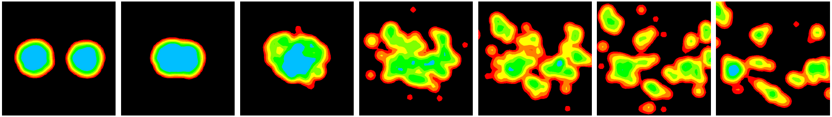

An event of central collision of Xe + Sn at 50 MeV/nucleon (AMD calculation)

Closely related through EOS

- Supernova
- Neutron Star

- Density ρ: $\cdots \sim \frac{1}{10}\rho_0 \sim \frac{1}{2}\rho_0 \sim \rho_0 \sim 2\rho_0 \sim \cdots$
- Temperature T: 0 MeV ~ 1 MeV ~ 10 MeV ~ ⋯
- Time scale: 10^{-22} s → 1 s (equilibrium)
- Number of particles: $10^2 \rightarrow 10^{??} = \infty$
- Neutron-proton asymmetry $\delta = \frac{N-Z}{A}$: 0 ~ 0.25 → 1

Nuclear EOS (at $T = 0$)

$$(E/A)(\rho_p, \rho_n) = (E/A)_0(\rho) + S(\rho)\delta^2 + \cdots$$

$$\rho = \rho_p + \rho_n, \quad \delta = \frac{\rho_n - \rho_p}{\rho_n + \rho_p}$$

- $S_0 = S(\rho_0)$ at the saturation density
- $L = 3\rho_0(dS/d\rho)_{\rho=\rho_0}$

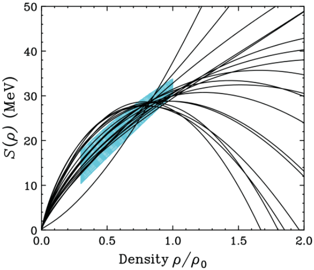

$S(\rho)$ for Skyrme interactions

Constrains on $S(\rho)$

Horowitz et al., J. Phys. G: Nucl. Part. Phys. 41 (2014) 093001.

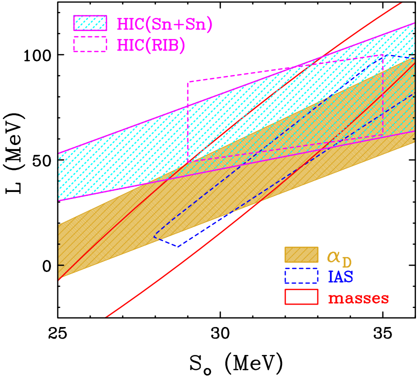

Symmetry energy from many approaches

Nuclear EOS (at $T = 0$)

$$(E/A)(\rho_p, \rho_n) = (E/A)_0(\rho) + S(\rho)\delta^2 + \cdots$$

$$\rho = \rho_p + \rho_n, \qquad \delta = \frac{\rho_n - \rho_p}{\rho_n + \rho_p}$$

- $S_0 = S(\rho_0)$ at the saturation density
- $L = 3\rho_0 (dS/d\rho)_{\rho=\rho_0}$

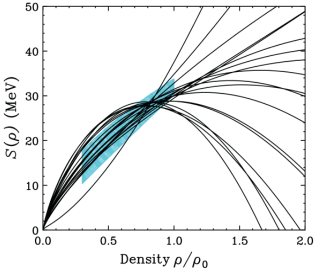

$S(\rho)$ for Skyrme interactions

Constrains on $S(\rho)$

Horowitz et al., J. Phys. G: Nucl. Part. Phys. 41 (2014) 093001.

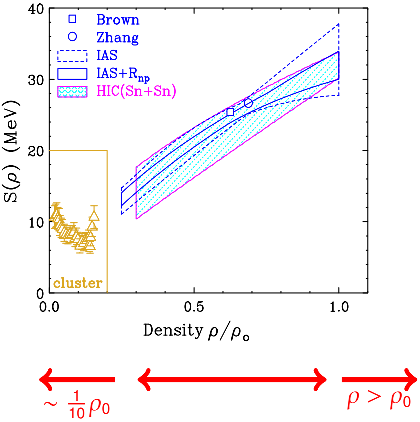

Clusters at low densities

Supernova

Abundance of light clusters in the post-bounce supernova core, based on nuclear statistical equilibrium.

Sumiyoshi and Röpke, PRC77 (2008) 055804.

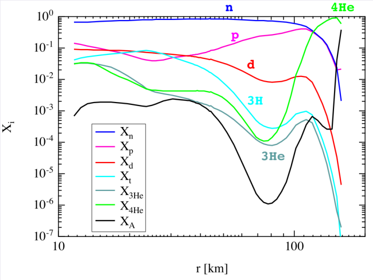

Heavy-Ion Collisions

Experimental data of cluster abundance in ^{36}Ar + ^{58}Ni for the events where the quasi-projectile is vaporized.

Borderie et al., EPJA6 (1999) 197, PLB388 (1996) 224.

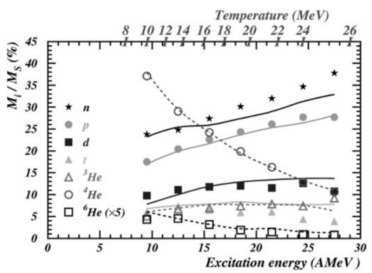

Linking Nuclear Matter and HIC

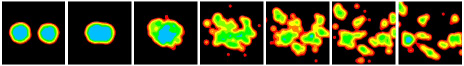

Nuclear Matter — EOS $P(\rho, \delta, T)$ ←···→ Heavy-Ion Collisions

Linking Nuclear Matter and HIC

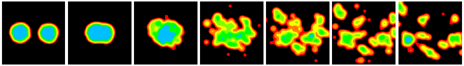

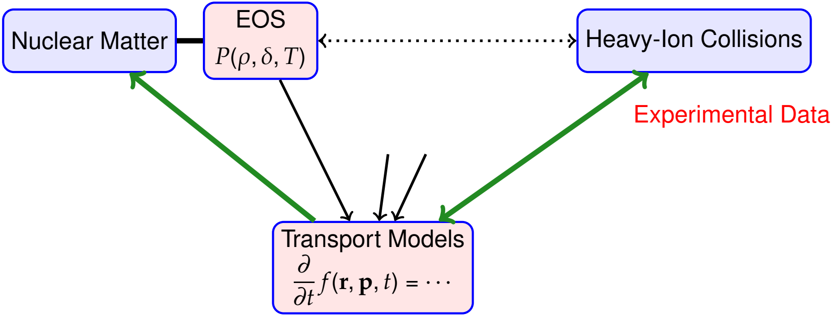

- Antisymmetrized Molecular Dynamics (AMD) — a transport model
- Application to heavy-ion collisions, to obtain information on EOS
- Possibility to apply to large systems, and to systems in thermal equilibrium

Antisymmetrized Molecular Dynamics

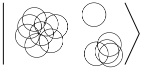

AMD wave function

$$|\Phi(Z)\rangle = \det_{ij}\Big[\exp\Big\{-\nu\Big(\mathbf{r}_j - \frac{\mathbf{Z}_i}{\sqrt{\nu}}\Big)^2\Big\}\chi_{\alpha_i}(j)\Big]$$

$$\mathbf{Z}_i = \sqrt{\nu}\mathbf{D}_i + \frac{i}{2\hbar\sqrt{\nu}}\mathbf{K}_i$$

ν : Width parameter = $(2.5\ \mathrm{fm})^{-2}$

χ_{α_i} : Spin-isospin states = $p\uparrow, p\downarrow, n\uparrow, n\downarrow$

Time-dependent variational principle

$$\delta\int_{t_1}^{t_2}\frac{\langle\Phi(Z)|(i\hbar\frac{d}{dt}-H)|\Phi(Z)\rangle}{\langle\Phi(Z)|\Phi(Z)\rangle}dt = 0, \qquad \delta Z(t_1) = \delta Z(t_2) = 0$$

Equation of motion for the wave packet centroids Z

$$\frac{d}{dt}\mathbf{Z}_i = \{\mathbf{Z}_i, \mathcal{H}\}_{\mathrm{PB}} \qquad \text{or} \qquad i\hbar\sum_{j=1}^{A}\sum_{\tau=x,y,z}C_{i\sigma,j\tau}\frac{dZ_{j\tau}}{dt} = \frac{\partial\mathcal{H}}{\partial Z_{i\sigma}}$$

Motion of wave packets in the mean field (c.f. $C_{i\sigma,j\tau} = \delta_{ij}\delta_{\sigma\tau}$ in QMD)

$$\mathcal{H} = \frac{\langle\Phi(Z)|H|\Phi(Z)\rangle}{\langle\Phi(Z)|\Phi(Z)\rangle} + (\text{c.m. correction}),$$

H: Effective interaction (e.g. Skyrme force)

Slater determinant of non-orthogonal wave functions

Slater determinant

$$\Phi_{\text{Slater}} = \mathcal{A}\Big[\varphi_1(\mathbf{r}_1)\varphi_2(\mathbf{r}_2)\cdots\varphi_A(\mathbf{r}_A)\Big]$$

The state represented by Φ is invariant under any regular linear transformation among the single-particle states $\{\varphi_1, \varphi_2, \ldots, \varphi_A\}$.

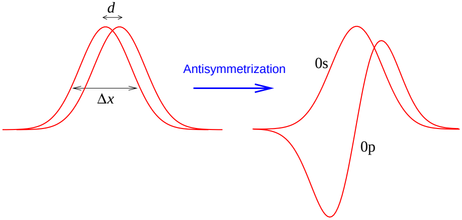

Many-body state represented by Φ_{Slater}

$\Updownarrow$

A-dim subspace of single-particle states

$\Updownarrow$

One-body density matrix ρ

$$\rho = \sum_{i=1}^{A}\sum_{j=1}^{A} |\varphi_j\rangle B^{-1}_{ji}\langle\varphi_i| \qquad \text{with} \quad B_{ij} = \langle\varphi_i|\varphi_j\rangle$$

Expectation value of a one-body operator

$O = o_1 + o_2 + \cdots + o_A$

$$\langle O\rangle = \mathrm{Tr}[o\rho] = \sum_{i=1}^{A}\sum_{j=1}^{A}\langle\varphi_i|o|\varphi_j\rangle B^{-1}_{ji}$$

Effective Interaction

Skyrme force, in recent calculations.

$$v_{ij} = t_0(1 + x_0 P_\sigma)\delta(\mathbf{r}) + \tfrac{1}{2}t_1(1 + x_1 P_\sigma)[\delta(\mathbf{r})\mathbf{k}^2 + \mathbf{k}^2\delta(\mathbf{r})] \qquad \mathbf{r} = \mathbf{r}_i - \mathbf{r}_j$$

$$+t_2(1 + x_2 P_\sigma)\mathbf{k}\cdot\delta(\mathbf{r})\mathbf{k} + t_3(1 + x_3 P_\sigma)[\rho(\mathbf{r}_i)]^\alpha\delta(\mathbf{r}) \qquad \mathbf{k} = \tfrac{1}{2\hbar}(\mathbf{p}_i - \mathbf{p}_j)$$

$$\langle V\rangle = \int \mathcal{V}\Big(\rho(\mathbf{r}), \tau(\mathbf{r}), \triangle\rho(\mathbf{r}), \mathbf{j}(\mathbf{r})\Big)d\mathbf{r} \qquad \sim A^2 \times \text{Volume}$$

$$\rho(\mathbf{r}) = \Big(\frac{2\nu}{\pi}\Big)^{\frac{3}{2}}\sum_{i=1}^{A}\sum_{j=1}^{A} e^{-2\nu(\mathbf{r}-\mathbf{R}_{ij})^2}B_{ij}B^{-1}_{ji}, \qquad \mathbf{R}_{ij} = \frac{1}{2\sqrt{\nu}}(\mathbf{Z}_i^* + \mathbf{Z}_j)$$

Finite-range effective interaction such as Gogny force

$$v_{ij} = \sum_{k=1,2}(W_k + B_k P_\sigma - H_k P_\tau - M_k P_\sigma P_\tau)e^{-(\mathbf{r}_i-\mathbf{r}_j)^2/a_k^2} + t_\rho(1 + P_\sigma)\rho(\mathbf{r}_i)^\sigma\delta(\mathbf{r}_i - \mathbf{r}_j)$$

$$\langle V\rangle = \frac{1}{2}\sum_{i=1}^{A}\sum_{j=1}^{A}\sum_{k=1}^{A}\sum_{l=1}^{A}\langle ij|v|kl - lk\rangle B^{-1}_{ki}B^{-1}_{lj} \qquad \sim A^4$$

Techniques for fast computation

Method by Sugawa and Horiuchi

Sugawa & Horiuchi, PTP105 (2001) 131

$$\rho(\mathbf{r}) = \left(\frac{2\nu}{\pi}\right)^{\frac{3}{2}} \sum_{i=1}^{A}\sum_{j=1}^{A} e^{-2\nu(\mathbf{r}-\mathbf{R}_{ij})^2} B_{ij}B_{ji}^{-1} = e^{-2\nu\mathbf{r}^2} \sum_{i=1}^{A}\sum_{j=1}^{A} C_{ij}(\mathbf{r}), \qquad C_{ij}(\mathbf{r}) = e^{-4\nu\mathbf{r}\cdot\mathbf{R}_{ij}} \times B_{ij}B_{ji}^{-1} e^{-2\nu\mathbf{R}_{ij}^2}$$

$C_{ij}(\mathbf{r})$ at different grid points are obtained by a geometric progression.

$$C_{ij}(\mathbf{r}+\mathbf{n}a) = C_{ij}(\mathbf{r})\, e^{-4\nu a\mathbf{R}_{ij}\cdot\mathbf{n}}$$

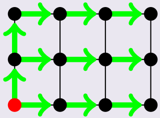

Cut-off by the spatial distance

To the density at a given point $\mathbf{r}$, the wave packets located very far from $\mathbf{r}$ do not contribute.

$$\rho(\mathbf{r}) = \left(\frac{2\nu}{\pi}\right)^{\frac{3}{2}} \sum_{i}^{|\mathbf{D}_i-\mathbf{r}|<R_0} \sum_{j}^{|\mathbf{D}_j-\mathbf{r}|<R_0} e^{-2\nu(\mathbf{r}-\mathbf{R}_{ij})^2} B_{ij}B_{ji}^{-1}, \quad R_0 \approx 10\text{ fm}$$

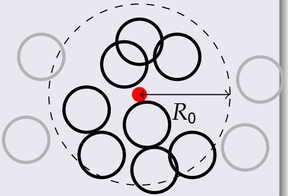

Combination of these two techniques.

Efficiency of numerical computation

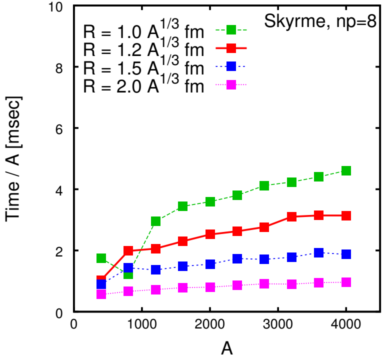

CPU time per nucleon for a computation of

$$\left\{ \frac{\partial}{\partial Z_k^*} \langle V \rangle; \quad k = 1, 2, \ldots A \right\}$$

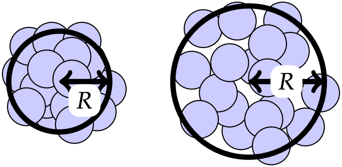

CPU time $\sim c(\rho) \times A^{1+\epsilon}$.

$c(\rho)$ is small for lower densities.

Xe + Sn central collisions at 50 MeV/nucleon

Without cluster correlations (AMD with NN collisions)

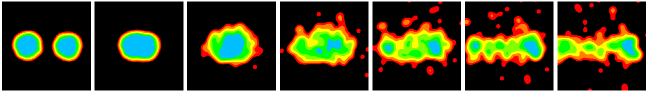

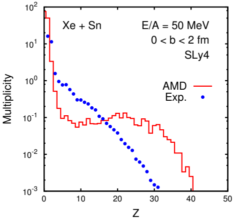

Two directions of extension of AMD

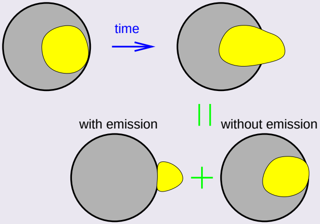

Wave-packet splitting: Give fluctuation to each wave packet centroid, based on the single-particle motion.

$$\frac{d}{dt}Z = \{Z, \mathcal{H}\}_{\mathrm{PB}} + \text{(NN Collision)}$$
$$+ \text{(W.P. Splitting)} + \text{(E. Conservation)}$$

AO and Horiuchi, PPNP53 (2004) 501

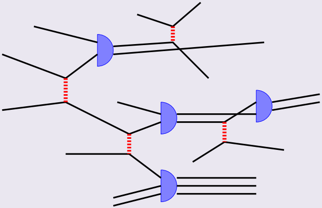

At each two-nucleon collision

$N_1 + B_1 \; + \; N_2 + B_2 \; \to C_1 + C_2$

$$v\rho\, d\sigma = \frac{2\pi}{\hbar}|\langle \mathrm{CC}|V_{NN}|\mathrm{NBNB}\rangle|^2 \delta(\mathcal{H} - E)\, p_{\mathrm{rel}}^2 dp_{\mathrm{rel}} d\Omega$$

AO, J. Phys. Conf. Ser. 420 (2013) 012103

Effect of Cluster and C-C Correlations

Xe + Sn central collisions at 50 MeV/nucleon

Without cluster correlations (AMD with NN collisions)

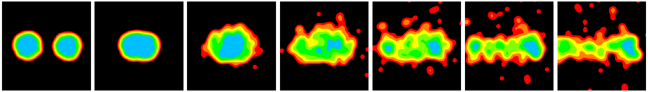

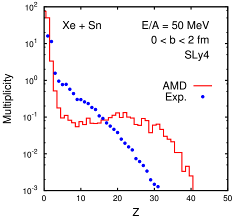

With cluster and cluster-cluster correlations

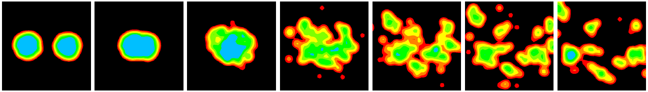

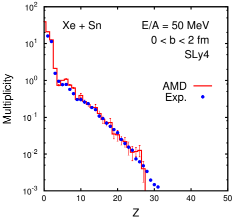

Model Comparison: Expansion followed by fragmentation

Colonna, Ono, Rizzo, PRC82 (2010) 054613.

- SMF = Stochastic Mean Field model
- AMD = Antisymmetrized Molecular Dynamics

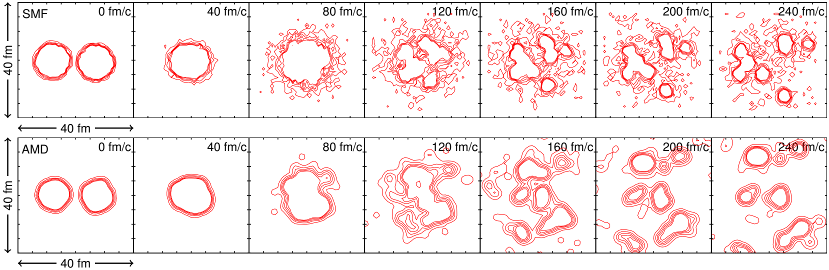

Central Collisions of ^{112}Sn + ^{112}Sn at 50 MeV/nucleon

Used the same σ_{NN} and very similar effective interactions in both models.

Efforts to understand the model differences are indispensable.

Rare isotope production by projectile fragmentation

Mocko, Tsang, AO et al., PRC78(2008)024612.

^{48}Ca + ^{9}Be at 140 MeV/nucleon

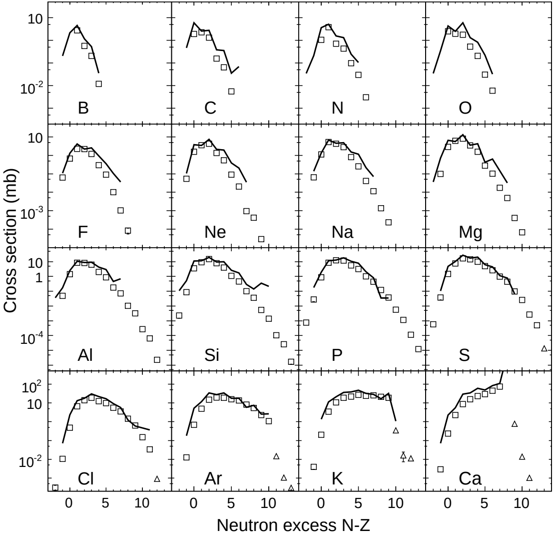

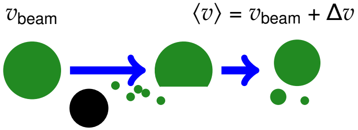

- AMD calc: 17,000 events
- Experiment: $\sim 10^7$ events

Is the equilibrium consistent with quantum statistics?

$$\frac{dZ}{dt} = \{Z, \mathcal{H}\}_{\text{PB}} + \Delta Z \qquad \Rightarrow \qquad \text{Equilibrium (Statistical Properties)}$$

Many related works by: Ono & Horiuchi, Ohnishi & Randrup, Schnack & Feldmeier, Sugawa & Horiuchi

Equilibrium Simulation

Solve long-time evolution for given volume V and energy E.

$\Rightarrow$ Microcanonical ensemble

$\Rightarrow$ (T, P)

$$\frac{1}{T} = \frac{\partial S(E)}{\partial E} = \left\langle \frac{\partial S_{\text{gas}}(E_{\text{gas}})}{\partial E_{\text{gas}}} \right\rangle_E$$

$$= \left\langle \frac{\frac{3}{2}N_{\text{gas}} - 1}{E_{\text{gas}}} \right\rangle_E \approx \frac{3}{2} \left\langle \frac{E_{\text{gas}}}{N_{\text{gas}}} \right\rangle_E^{-1}$$

Furuta and Ono,
PRC79 (2009) 014608;
PRC74 (2006) 014612.

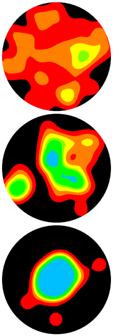

Constant pressure caloric curves

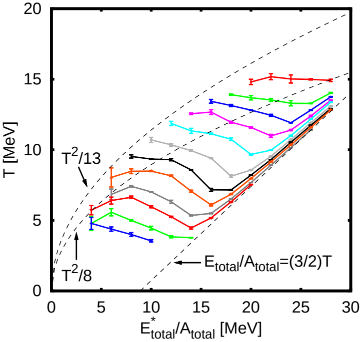

Liquid-gas phase transition

Comparison of reaction and equilibrium

^{40}Ca + ^{40}Ca, E/A = 35 MeV, b = 0

Furuta and Ono, PRC79 (2009) 014608.

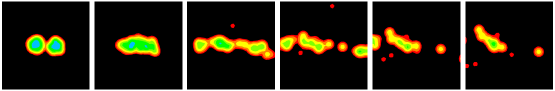

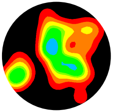

$\{$States at a reaction time $t\}$ $\overset{?}{=}$ An equilibrium ensemble ($E, V, A = 36$)

half of Ca + Ca system

t = 100 fm/c 140 fm/c 180 fm/c 300 fm/c

$Y(Z)$

$\langle E^*/A \rangle$

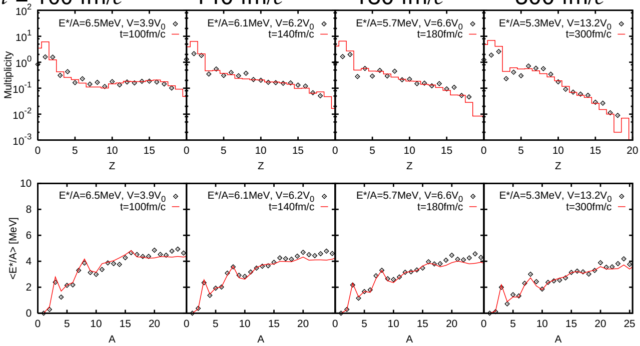

Liquid-Gas separation in fragmentation reactions

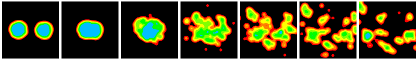

At a late stage of reaction

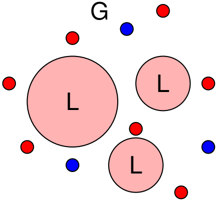

Fractionation/Distillation/蒸留

$$\delta(\text{liquid}) < \delta(\text{gas}), \qquad \delta = \frac{N-Z}{N+Z}$$

- Gas = $\sum(A \le 4 \text{ particles})$
- Liquid = $\sum(A > 4 \text{ fragments})$
- Total = Gas + Liquid

Isospin asymmetry of the liquid part δ_{liq} in ^{124}Sn + ^{124}Sn and ^{112}Sn + ^{112}Sn central collisions at 50 MeV/nucleon.

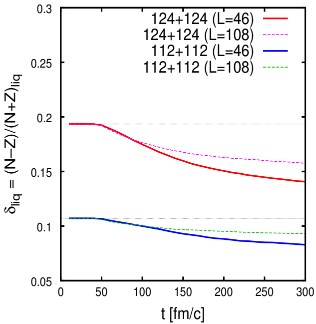

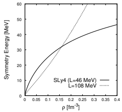

Fractionation is strong for soft symmetry energy. (⇔ Low-density effect)

Energy spectra of clusters (t and ^{3}He)

^{124}Sn + ^{124}Sn and ^{112}Sn + ^{112}Sn central collisions at 50 MeV/u ($60^\circ < \theta_{cm} < 120^\circ$)

SLy4 (L = 46 MeV)

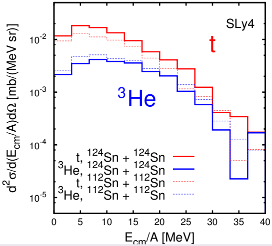

L = 108 MeV

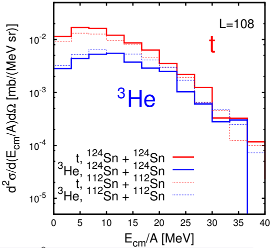

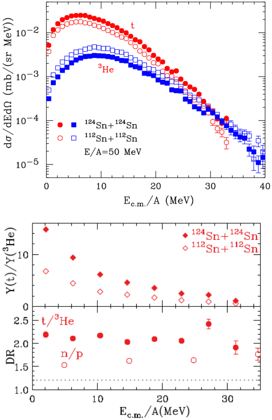

$Y(t)/Y(^3\mathrm{He})$ ratio for ^{124}Sn + ^{124}Sn	$L = 46$	$L = 108$
$E/A < 10$ MeV	4.76	3.57
$E/A > 20$ MeV	2.25	1.65

Consistent with the low-density EOS.

Liu et al., PRC86(2012)024605.

For the symmetry energy at high densities $\rho \sim 2\rho_0$.

^{132}Sn + ^{124}Sn collisions at 300 MeV/nucleon, $b < 2$ fm

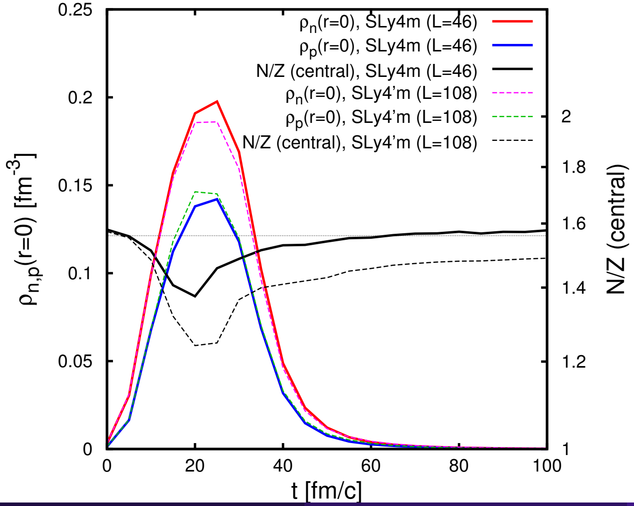

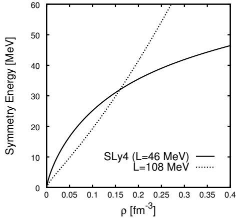

"central": within a radius from the center of mass of the system that contains 25 % of the total nucleons.

Dynamics in Compression and Expansion

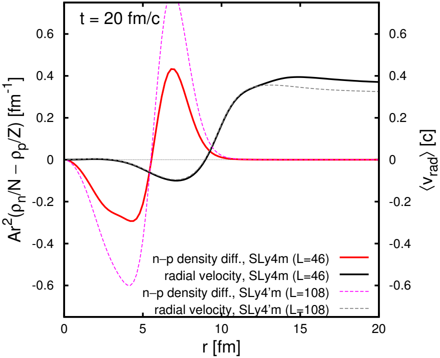

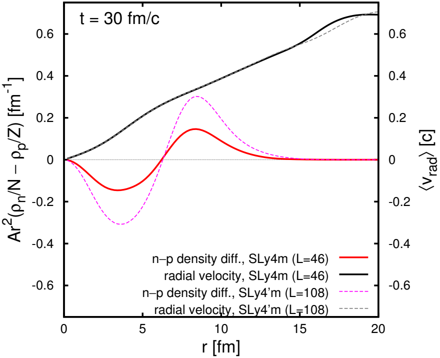

- Difference of angle-averaged densities, $\rho_n(r)$ and $\rho_p(r)$
- Averege radial velocity $v_{\text{rad}}(r)$

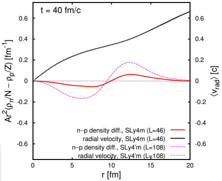

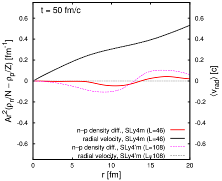

The effect at compression remains until later times.
⇒ In observables?

N/Z Spectrum Ratio — an observable

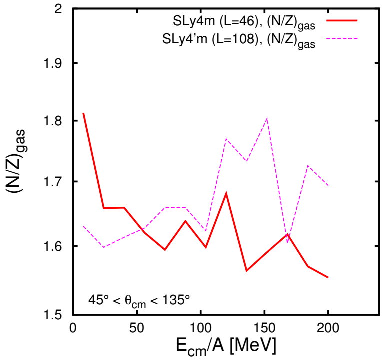

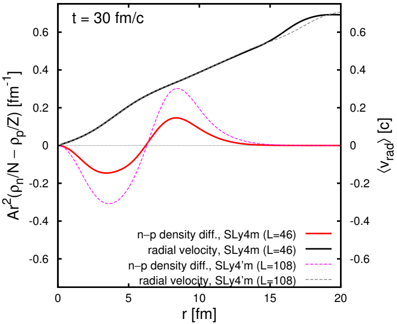

$$\left(\frac{N}{Z}\right)_{\text{gas}} = \frac{Y_n(v) + Y_d(v) + 2Y_t(v) + Y_h(v) + 2Y_\alpha(v)}{Y_p(v) + Y_d(v) + Y_t(v) + 2Y_h(v) + 2Y_\alpha(v)}$$

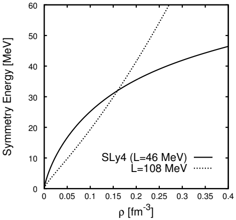

The N/Z spectrum ratio seems similar to the difference of $\rho_n(r)$ and $\rho_p(r)$ in the early stage.

Composition and Spectra of Clusters

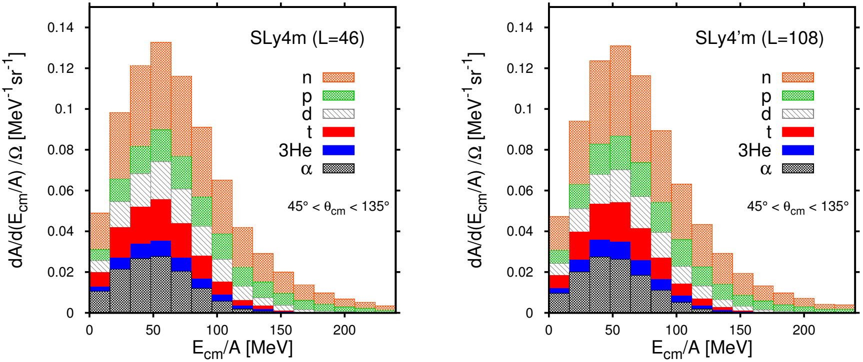

Summary

Toward a unified description of nuclear collision dynamics and nuclear matter.

- Application to heavy-ion collisions and comparison with experimental data.
  - Improvement of transport models. e.g., cluster correlations.
  - Getting information of EOS. Symmetry energy at various densities.
- Application to systems in thermal equilibrium.
  - Liquid-gas phase transition in finite systems.
  - Tuning the model and the code for large systems.